The Journal of Experimental Biology 213, 3699-3704

doi:10.1242/jeb.047654

Changes in materials properties explain the effects of humidity on gecko adhesion

Jonathan B. Puthoff[1], Michael S. Prowse[2], Matt Wilkinson[1] and Kellar Autumn[1,2,*]

[1]Department of Biology, Lewis and Clark College, 0615 Palatine Hill Road, Portland, OR 97219-7899, USA and [2]Materials Science and Engineering Department, University of Washington, 302 Roberts Hall, Seattle, WA 98195-2120, USA

*Author for correspondence (autumn@lclark.edu)

Accepted 9 August 2010

SUMMARY

Geckos owe their remarkable stickiness to millions of dry setae on their toes, and the mechanism of adhesion in gecko setae has been the topic of scientific scrutiny for over two centuries. Previously, we demonstrated that van der Waals forces are sufficient for strong adhesion and friction in gecko setae, and that water-based capillary adhesion is not required. However, recent studies demonstrated that adhesion increases with relative humidity (RH) and proposed that surface hydration and capillary water bridge formation is important or even necessary. In this study, we confirmed a significant effect of RH on gecko adhesion, but rejected the capillary adhesion hypothesis. While contact forces of isolated tokay gecko setal arrays increased with humidity, the increase was similar on hydrophobic and hydrophilic surfaces, inconsistent with a capillary mechanism. Contact forces increased with RH even at high shear rates, where capillary bridge formation is too slow to affect adhesion. How then can a humidity-related increase in adhesion and friction be explained? The effect of RH on the mechanical properties of setal β-keratin has escaped consideration until now. We discovered that an increase in RH softens setae and increases viscoelastic damping, which increases adhesion. Changes in setal materials properties, not capillary forces, fully explain humidity-enhanced adhesion, and van der Waals forces remain the only empirically supported mechanism of adhesion in geckos.

Key words: gecko, adhesion, van der Waals, capillary force, materials properties.

INTRODUCTION

The superlative climbing skill of geckos has been remarked upon since antiquity (Aristotle, 1910), but only recently have the fundamental principles underlying their scansorial abilities been revealed (Autumn et al., 2000; Autumn and Peattie, 2002; Autumn et al., 2002; Russell, 2002). The gecko attachment system is built on a hierarchy of length scales in the structures of the feet (Federle, 2006; Autumn and Peattie, 2002; Maderson, 1964; Ruibal and Ernst, 1965), which are composed primarily of β-keratin (Fraser and Macrae, 1980; Fraser and Parry, 1996; Maderson, 1964; Rizzo et al., 2006). At the smallest scales, the compliant spatulae afford the creature the ability to bring its digits into intimate contact with the roughest of surfaces (Huber et al., 2007; Russell and Johnson, 2007). These spatulae are bundled into stiffer setae (Rizzo et al., 2006), which are packed densely on lamellae of the toe (Russell, 2002). At the scale of the toe and foot, the lizard can adjust the angle that these setal arrays make with the surface; at some critical angle, the setae detach spontaneously (Autumn et al., 2006a; Autumn et al., 2000; Yamaguchi et al., 2009). The incorporation of exclusively 'dry' components (Autumn et al., 2002), a quick-release mechanism (Russell, 2002), near-indefinite reusability, and self-cleaning (Hansen and Autumn, 2005) make gecko adhesion mechanics interesting not just to researchers in the natural sciences but also to those in engineering disciplines. There are numerous research programs aimed at fabricating gecko-like synthetic adhesives (GSAs) that reproduce the important features of the gecko system (Autumn et al., 2002; Geim et al., 2003; Lee et al., 2009; Mahdavi et al., 2008; Murphy et al., 2007; Sitti and Fearing, 2003).

The adhesive capabilities of the gecko are the result of a vast number of nanoscale contacts between the spatulae and the terrain. The fact that geckos can climb on atomically smooth surfaces (Autumn et al., 2002; Sitti and Fearing, 2003) is an indication that interlocking of the appendages in crevices on the surface is not required for adhesion. Nor do electrostatic forces appear to be necessary (Dellit, 1934). Intermolecular van der Waals (vdW) forces are sufficient to explain the stickiness of the foot structures (Autumn et al., 2002), although there has been speculation that other effects may modify (or even dominate) vdW adhesion. One proposed mechanism is capillary condensation, which is adsorbed atmospheric moisture at the points of contact (Thomson, 1871). This adsorbed moisture will influence the adhesion between bodies under humid conditions (McFarlane and Tabor, 1950) even at small (nm) length scales (Fisher and Israelachvili, 1981). Capillary bridges between and around two asperities in contact will contribute to the adhesive forces between them because of the well-known Laplace pressure effect, provided that the surface tension of the water is smaller than the surface free energy of the solids (i.e. the surfaces are hydrophilic). For some organisms, such as tree frogs (Federle et al., 2006; Hanna and Barnes, 1991), the capillary action of native mucus plays an important role in the animal's climbing capability.

The influence of humidity on the adhesion of geckos has been investigated at the spatular level (Huber et al., 2005; Sun et al., 2005), the organism level (Niewiarowski et al., 2008) and with a multi-scale model (Kim and Bhushan, 2008). Sun and colleagues reported an apparent capillary influence on spatula adhesion, indicated solely by large increases in adhesive force values on hydrophilic substrates in a highly humid environment (Sun et al., 2005). In a publication nearly simultaneous with that of Sun et al. (Sun et al., 2005), Huber and colleagues presented measurements of spatular adhesion that increase continuously with humidity on a hydrophilic substrate (Huber et al., 2005). The Huber study is also notable for the accompanying experiments performed on a hydrophobic surface, which showed a similar, if smaller, continuous increase in adhesion with humidity. Niewiarowski and colleagues

observed enhanced adhesion at high humidity (Niewiarowski et al., 2008), though the observed temperature dependence of the forces in their study is difficult to interpret. Kim and Bhushan modeled these effects and made some useful calculations of the magnitude of capillary forces for contact between elements with varying degrees of hydrophobicity/hydrophilicity (Kim and Bhushan, 2008).

These studies raise questions about the exact interplay between the different adhesive forces at work in the gecko system, a topic of central importance in the study of the gecko climbing system and in the design of bio-inspired synthetic adhesives. Why did the results of Huber and colleagues (Huber et al., 2005) show a continuous increase in adhesion with humidity, rather than a 'step' corresponding to capillary bridge formation between their single spatula and the substrate, as predicted by Sun and colleagues (Sun et al., 2005)? Why do the experiments on hydrophobic substrates show enhanced adhesion, when Laplace pressure forces between hydrophobic materials are expected to produce a repulsive contribution [see p. 331 of Israelachvili (Israelachvili, 1992)]? The data of Huber and colleagues (Huber et al., 2005) do not fit a capillary bridge model and these authors suggested that the enhanced forces are the result of a modification of the van der Waals forces by an intermediate water layer. Additionally, there is evidence that dry, hydrophobic setal arrays become more hydrophilic with exposure to water (Pesika et al., 2009), though these effects appear to be quite small.

Here, we reconcile the conflicting theory and data of the effects of van der Waals forces and humidity on gecko adhesion. We propose that there is another, untested effect of atmospheric moisture: modification of the mechanical properties of the β-keratin that setae are made of (Chen and Gao, 2010). Some recent progress has been made in understanding the influence of the materials properties of the appendages on insect (Goodwyn et al., 2006) and gecko adhesion (Autumn et al., 2006b; Persson, 2003). The mechanical properties of β-keratin have been subjected to some scrutiny, and a number of studies (Bonser, 2002; Bonser and Purslow, 1995; Fraser and Macrae, 1980; Taylor et al., 2004) have determined that the deformation properties of these keratins are sensitive to the degree of hydration. This fact provides an alternative explanation of how RH affects the gecko system: a softened spatula should be capable of conforming more closely to an underlying surface, enhancing vdW adhesion.

We investigated the plausibility of a capillary adhesion effect using two complementary approaches. We measured the effect of RH on contact forces (i) for both hydrophilic and hydrophobic substrates and (ii) for shear rates that span the expected timescale of capillary bridge formation. The forces produced by water menisci depend on the geometry of the capillary bridge, which in turn depends on the respective surface energies of the materials in contact. We explored these effects by selecting substrates at opposite ends of the surface energy spectrum: a hydrophilic surface, which has a contact angle $\theta<90$ deg, and a hydrophobic surface with $\theta>90$ deg. With respect to (ii), consider that the formation time t_{cap} of water bridges is fixed by the atmospheric conditions and contact geometry, while drag velocity determines the lifetime τ of the bridges. These two competing kinetic phenomena will produce a strong rate effect in the adhesion measurements. The characteristic timescale for capillary disintegration can be estimated for our system as:

$$\tau = \frac{\text{Spatula slip length}}{\text{Drag velocity}} . \quad (1)$$

When the capillary formation time t_{cap} (constant at all velocities) is small compared with τ, meniscus formation saturates and the capillary contribution to adhesion will be significant. When $\tau<t_{cap}$, bridges are unable to form and capillary contributions to adhesion will be negligible.

In addition to the experiments aimed at identifying capillary effects in the adhesion of gecko setae, we also investigated the effects of RH on the mechanical properties of setal β-keratin using dynamic mechanical analysis (DMA). These experiments on tissue properties, when combined with the substrate and rate experiments outlined above, allow us to test four hypotheses.

Hypothesis 1 (humidity effect on contact force): adhesion and friction will increase with RH.

Hypothesis 2 (substrate effect on capillary adhesion): RH effects will be greater on hydrophilic surfaces than on hydrophobic surfaces.

Hypothesis 3 (rate effect on capillary adhesion): RH effects will be reduced at high shear rates, where capillary bridges have insufficient time to form.

Hypothesis 4 (humidity effect on materials properties): setae will become softer and more tacky at high RH.

Hypotheses 1–3 are consistent with a capillary mechanism of adhesion. Hypothesis 4 represents an unexplored aspect of biological adhesion; namely, that changes in the materials properties of the tissue with atmospheric moisture can influence adhesion.

MATERIALS AND METHODS

Setal array specimens were collected from the scansors of live, adult tokay geckos (*Gekko gecko* L.) and mounted on aluminium stubs with cyanoacrylate glue. Arrays can be isolated without harm from unanesthetized geckos. Using previous methods (Autumn et al., 2002), we peeled the setal backing layer away from the lamella. The animal's loss of adhesive function in this digit is recovered at the next molt. Friction and adhesion experiments were conducted on a custom-made mechanical testing platform ('Robotoe') (Gravish et al., 2008), incorporating a 2-axis positioning stage (Aerotech, Pittsburg, PA, USA), piezoelectric load cell (Kistler, Amherst, NY, USA) (with a resolution of 1.3 and 2.6 mN in shear and normal forces, respectively), and a controlled-environment enclosure. During a single test, the mounted setal arrays are dragged across the substrate in a manner reminiscent of a gecko footfall (Gravish et al., 2008). We performed drag tests at five different RH levels (RH=10, 25, 50, 60, 70, and 80%) at five different drag velocities (v=5, 11, 22, 47, 100 μm s^{-1}) on two different substrates [silica glass microscope slides (various laboratory suppliers) and gallium arsenide (GaAs) wafers (American Xtal Technology, Fremont, CA, USA)]. Humidity in the chamber was stabilized at a low level (10% RH), then slowly ramped upward with a constant-RH soak of 0.5 h at each RH prior to testing. We confirmed that the silica glass was hydrophilic (θ=42±2 deg) and that the GaAs wafer was hydrophobic (θ=105±2 deg) with optical measurements.

We cut strips of the smooth, outer epidermal layer from setal arrays that were collected in the same manner as above. One end of each strip was affixed with cyanoacrylate glue to a glass laboratory slide mounted on the positioning stage. The free end of the attached keratin strip was then brought into contact with a spot of glue on a single axis force sensor. DMA testing produces viscoelastic properties data for a specimen subjected to a sinusoidal strain with amplitude ε_0 and frequency ω: $\varepsilon(t)=\varepsilon_0\sin(\omega t)$. The resulting dynamic stress $\sigma(t)=\sigma_0\sin(\omega t+\delta)$ will be phase shifted with respect to the strain by the loss angle δ. The dynamic material behavior can be described by the magnitude of the complex modulus E:

$$|E| = \sqrt{(E')^2 + (E'')^2} = \frac{\sigma_0}{\varepsilon_0} , \quad (2)$$

where the moduli E' and E'' are the real and imaginary parts of E, respectively, and the loss tangent:

$$\tan\delta = \frac{E''}{E'} . \quad (3)$$

We conducted our tests at three different frequencies (ω=0.5, 5 and 10 Hz), over a range of humidity (RH=10, 20, 30, 40, 50, 60, 70 and 80%), and at nominal ε_0=2%.

RESULTS

The adhesion/friction *vs* RH data obtained from the isolated setal arrays on the two different substrates are shown in Fig. 1. Fig. 1 also contrasts the behavior of arrays dragged at different velocities on each substrate. Consistent with Hypothesis 1, adhesion (Fig. 1A) and friction (Fig. 1B) increased with RH at all velocities. In contradiction to Hypothesis 2 (capillary adhesion, substrate effect), the effect of RH did not differ significantly between tests conducted on hydrophilic and hydrophobic surfaces. The data in Fig. 1A contradict Hypothesis 3 (capillary adhesion, rate effect), as well. For a slip length of ~100 nm (Gravish et al., 2010), a range of v=5–100 μm s^{-1} indicates that τ=1–20 ms from Eqn 1. Nanoscale capillary formation times have been estimated from atomic force microscopy measurements as t_{cap}=4.2 ms (Szoszkiewicz and Riedo, 2005). Comparing this value of t_{cap} to the range of τ represented in our experiment, we see that our data span the timescale where we would expect to observe strong rate effects, exemplified by larger adhesion values at lower test velocities. An inspection of the data in Fig. 1A indicates the opposite trend; adhesion is greater at higher drag velocities.

Fig. 2 shows the results of the DMA experiments on the setal β-keratin. The effects of moisture on the materials properties, typified by the magnitude of the complex modulus $|E|$ and the loss tangent tanδ, are apparent from Fig. 2; a decrease in modulus occurred as the humidity increased, and the effect was reversed for tanδ. This indicates that the storage modulus E' decreased significantly. This behavior is consistent with previous studies on the deformation of avian β-keratin (Bonser, 2002; Bonser and Purslow, 1995; Fraser and Macrae, 1980; Taylor et al., 2004), which showed that the storage modulus can decrease by as much as 95% at high humidity (Taylor et al., 2004). A decrease in E' relative to the loss modulus E'' results in a material with a larger time-dependent (viscous) deformation component. Hence, humidity softened the setal keratin and made it more tacky, consistent with Hypothesis 4.

DISCUSSION

The aim of this study was to determine whether and how RH affects adhesion in gecko setae, and to resolve the controversy over whether capillary adhesion plays a significant role in these effects. We confirmed that an increase in RH causes an increase in adhesion and friction in isolated gecko setal arrays (Hypothesis 1). However, in contradiction to a capillary mechanism, we measured a similar humidity-mediated increase in contact forces on hydrophilic and hydrophobic surfaces (rejecting Hypothesis 2). The enhanced adhesion that occurs with increased RH on the hydrophobic GaAs surface cannot be the result of capillary bridges between the substrate and the terminal surfaces of the setal array, because formation of capillary bridges would actually reduce adhesion [see p. 331 of Israelachvili (Israelachvili, 1992)]. Furthermore, shear rates too high to permit capillary condensation did not produce a decline in forces at high RH (rejecting Hypothesis 3). Taken together, these results suggest strongly that capillary forces do not have a significant influence on gecko adhesion and cannot explain the increase in contact forces with RH.

What then is the cause of the observed humidity effects on gecko adhesion? It is well known that the stiffness (Bonser, 2002; Bonser and Purslow, 1995; Fraser and Macrae, 1980; Taylor et al., 2004) and damping (Danilatos and Postle, 1981) of structural proteins such as keratins are affected strongly by humidity, and our DMA results show that gecko setal β-keratin is no exception (Hypothesis 4). An

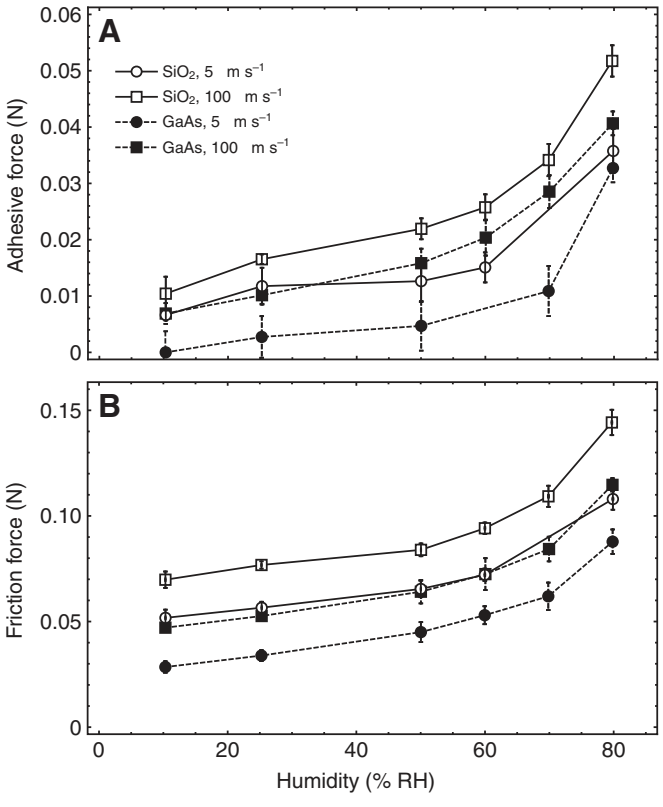

Fig. 1. The influence of velocity and humidity on the (A) adhesion and (B) friction of isolated gecko setal arrays during steady-state drag. Each symbol is the mean of a group of trials (N=6); the error estimates are the standard error of each group. The data have been shifted upward by a constant force (6.4 mN) to correct for an apparent offset during initial specimen positioning.

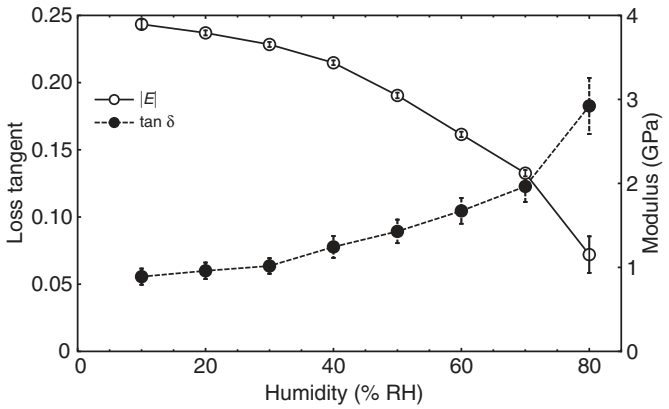

Fig. 2. The viscoelastic parameters from the dynamic mechanical analysis (DMA) experiments, measured at different humidity levels. A drop in the complex modulus $|E|$ concurrent with a rise in the loss tangent tanδ is indicative of a drop in the storage modulus E'. Each data point is the mean of a number of trials (N=9); the error bars represent the standard error for each set of trials.

increase in RH from 10% to 80% produced a decrease in the elastic modulus of 75% and a 4-fold increase in loss tangent; this indicates the keratin has become a softer and more viscous material. Since we know that the dissipative effects associated with viscoelasticity influence adhesion (Kendall, 1979), we can explore how RH affects the gecko system with a materials-based model of interface fracture based on the Griffith concept (Griffith, 1921). First, we derive a detachment condition that relates the adhesive pull-off force F_a to the geometrical and material properties of the adhered body. When the expected humidity dependence of these different factors is inserted, we arrive at a relationship that can be used to interpret the data in Figs 1 and 2.

Fracture model of interface toughness

The fracture model of adhesion is based on the release of stored elastic energy in a body as it peels from a substrate. Consider the flat-tipped, cylindrical fiber of radius R peeling from a surface shown in Fig. 3. Under the influence of the applied stress σ, the adhered bodies will deform and store elastic energy, like a spring. This energy, which is related to their elastic constants (storage modulus E' and Poisson's ratio ν), will be released as they separate. Conservation principles dictate that there is a cost to expanding the cracked region, however. This cost is the work of adhesion γ (with units of work/area), which reflects the energy change in the system associated with creating new surface area and, in the simplest case, is related to the strength of the vdW bonds between the two bodies. When these two competing energetic contributions are balanced, a detachment criterion can be described by (Gao and Yao, 2004; Gao et al., 2005):

$$\sigma_a = \sqrt{\frac{8E^*\gamma}{\pi R}} , \quad (4)$$

where σ_a is the critical stress to achieve pull-off and E^* is the contact modulus given by $[(1-\nu^2)/E'+(1-\nu_{substrate}^2)/E'_{substrate}]^{-1}$ (think of two springs in series).

For materials with a substantial viscous component to deformation there will be additional energy dissipated by inelastic mechanisms in the bodies themselves, far from the crack tip. Consequently, the energy balance for adhesion will be modified slightly. The work of adhesion has two components in this case, one representing the intermolecular attraction γ_0 and the other representing viscoelastic losses to the system $\Delta\gamma$, or:

$$\gamma = \gamma_0 + \Delta\gamma(\tan\delta, v_c) , \quad (5)$$

where $\Delta\gamma$ is shown explicitly as a function of the viscoelastic parameter $\tan\delta$ and the crack extension velocity v_c. Existing theories (Andrews, 1985; Hui et al., 1992; Saulnier et al., 2004) for the effect of viscoelasticity on the work of adhesion take $\Delta\gamma=\gamma_0\Phi(\tan\delta, v_c)$, i.e. the influence of viscoelastic/rate effects is through a multiplicative function Φ that includes the viscoelastic and rate terms. Using this and Eqn 5, we can represent the modification of detachment behavior by viscoelastic and rate effects on adhesion force as:

$$F_a = A\sqrt{\frac{8E'(\gamma_0+\Delta\gamma)}{\pi R(1-\nu^2)}} = \sqrt{\frac{8\pi R^3E'\gamma_0(\Phi+1)}{(1-\nu^2)}} , \quad (6)$$

where we have used the relation $F_a=\sigma_aA=\sigma_a\pi R^2$ (where A is the cross-sectional area) and the simplifying assumption that the substrate is very stiff compared with the fiber, i.e. $E^*\approx E'/(1-\nu^2)$.

Humidity dependence and rate dependence of pull-off force

Eqn 6 gives some indication of how the humidity influences the adhesive forces. There are three factors that we expect to depend on the humidity: the geometric (R), as a result of swelling; the elastic (E'), as a result of softening; and the viscoelastic ($\tan\delta$), as a result of enhanced dissipation. Rewriting Eqn 6 using the definition $F_0=\sqrt{[8\pi\gamma_0/(1-\nu^2)]}$ for the humidity-independent factors gives $F_a=F_0\sqrt{\{R^3E'[\Phi(\tan\delta,v_c)+1]\}}$. Note that by reformatting the pull-off force like this, we have segregated it into substrate-dependent (F_0) and substrate-independent factors.

The precise humidity dependence of the geometric, elastic and viscoelastic parameters are *a priori* unknown, but we can explain humidity effects using a simple heuristic argument that is based on the scaling behavior of the individual variables. For example, the adhered fiber in Fig. 3 has a cross-section that scales as $A\propto R^2$. Because an increase in A produces a decrease in the applied stress σ, the interface between the materials will be effectively toughened as R increases. Assuming linear swelling with moisture in this dimension gives $R\propto$RH. Next, following Saulnier et al. (Saulnier et al., 2004), we take the β-keratin to be a 'soft solid' and therefore have $\Phi\propto v_c\tan^2\delta$. As $\tan\delta\propto(E')^{-1}$ (cf. Eqn 3), the pull-off force in Eqn 6 will vary overall as $(E')^{-1}$. The dependence of E' on humidity can be assumed for now as $(E')^{-1}\propto(\mathrm{RH})^m$, where $m>1$ (cf. Fig. 2). Finally, as the crack extension velocity v_c is parallel to the drag velocity v enforced by our experiment, they are roughly analogous. We can now write:

$$\sqrt{R^3E'\left(\Phi+1\right)} \propto \sqrt{v}\left(\mathrm{RH}\right)^{\frac{3+m}{2}} , \quad (7)$$

which is a simple expression illustrating how the humidity-dependent part in Eqn 6 is expected to behave as RH increases.

The exponent $(3+m)/2$, henceforth ζ, describes the highest-order effect of humidity on the adhesive force, and will dominate the behavior at high RH. The final expression for the pull-off force as a function of humidity and velocity may be written as:

$$F_a = \alpha F_0\sqrt{v}\left(\mathrm{RH}\right)^{\zeta} + o\left(\mathrm{RH}, v\right) , \quad (8)$$

where α is the coefficient of the highest-order term in (RH,v) and the function o is composed exclusively of terms that are asymptotically small. Note that the form of Eqn 8 does not exclude

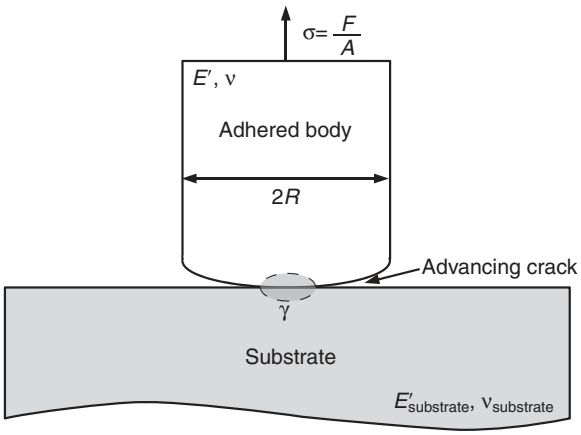

Fig. 3. Schematic diagram of fibril detachment by interfacial fracture. The separation of the two elastic bodies proceeds by the expansion of the separated region between them. This expansion is driven by stored elastic energy, which depends on the stress state and the elastic moduli, and inhibited by the interfacial bonding, the strength of which is determined by the work of adhesion term γ. The variables E', fiber radius R and γ are all expected to vary with relative humidity RH. Here, A is the cross-sectional area, F is the applied force, ν is Poisson's ratio and σ is the stress applied to the fiber.

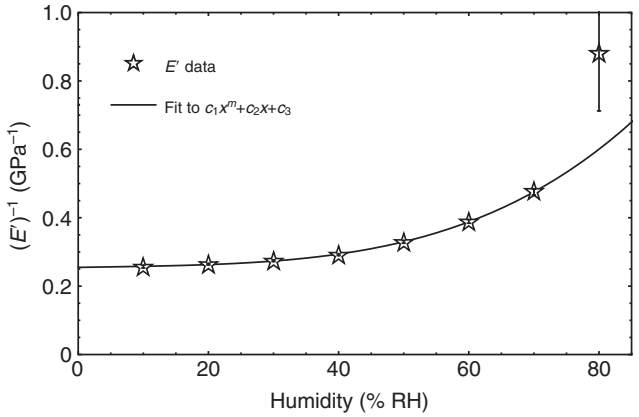

Fig. 4. The relationship between storage modulus and humidity. The superimposed non-linear fit gives the scaling relationship $(E')^{-1} \propto (\mathrm{RH})^{3.6}$. The error bars are the result of error propagation from the data in Fig. 2.

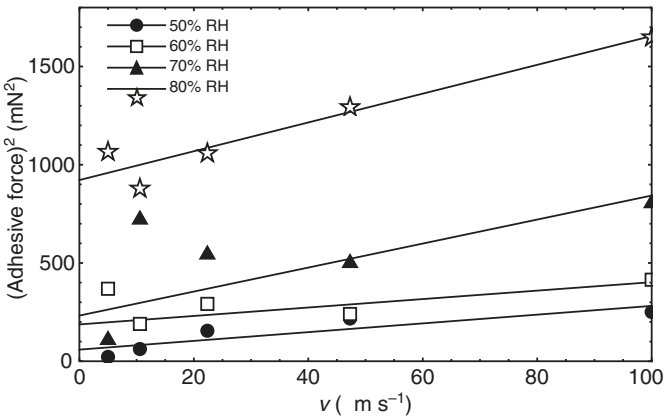

Fig. 6. Scaling of adhesive forces (F_a) with velocity. When (adhesive force)^2 is plotted against v, linear behavior results, confirming the relationship $F_a \propto v^{1/2}$.

an additional, linear increase in vdW dispersion forces with humidity as proposed by Huber and colleagues (Huber et al., 2005). It indicates, rather, that at high RH the viscoelastic contribution to adhesion will be the dominant effect.

Analysis of adhesion and friction data

The form of Eqn 8 describes adequately the trends of the data in Fig. 1A. The data in Fig. 4, which were derived from those in Fig. 2, show the dependence of $(E')^{-1}$ on humidity. From a non-linear fit to this series, we estimate m=3.6±0.2. For this value of m, ζ=3.3±0.1. This exponent is in agreement with the shape of the adhesive force *vs* humidity curves at all velocities. To illustrate this, we have placed all of the adhesion force curves collected on the GaAs substrate on log–log axes in Fig. 5. A linear fit to the high humidity (RH>60% or so) portions of each of these series allows us to determine the exponent ζ_{GaAs}. The aggregate data in Fig. 5 indicate that ζ_{GaAs}=3.0±0.2. A similar analysis for the SiO_2 series gives ζ_{SiO_2}=2.8±0.2. The values of ζ_{GaAs} and ζ_{SiO_2} are similar, which is what we would expect for substrate-independent behavior. They are, however, a bit smaller than we would expect from our calculated value of ζ. Further confirmation of the validity of Eqn 8 is shown in Fig. 6, which is a plot of (adhesion force)^2 *vs* test velocity for the data collected on GaAs at a number of humidity levels. Despite some noise at low v values, the linear trends of these series indicate that adhesive force$\propto\sqrt{v}$.

Note that Eqn 8 does not include the effects of changes in surface properties resulting from internal rearrangement of the proteins (Pesika et al., 2009). We expect the alteration of surface properties to influence the short-range parameter γ_0, so our estimate of the exponent ζ is subject to error in this respect. This effect could account for the discrepancy with our measured values. However, we know that the change in surface energy is quite small over the range 0–100% RH (Pesika et al., 2009). There are also complicating effects that are the result of the fibrillar structure of the arrays which need to be included in any complete model of gecko adhesion, but the agreement of the asymptotic force law of Eqn 8 with our array data is quite encouraging. It is not unreasonable to assume a simple multiplicative effect for some large number of adhered structures.

Finally, the increased adhesion has implications for the friction force F_f between the gecko's foot and the substrate. A simple formula that incorporates the enhanced adhesion is:

$$F_f = \mu\,(F + F_a)\,, \tag{9}$$

where F is the applied force and μ is the (macroscopic) coefficient of friction. Eqn 9 explains the approximately proportional increase in friction with adhesion that can be seen in Fig. 1.

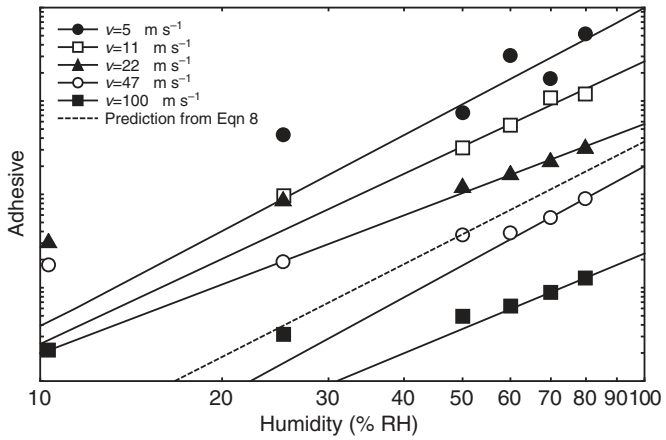

Fig. 5. Power law fits of adhesion data on GaAs at all velocities (v). (The vertical position of each curve has been adjusted, for the sake of clarity.) From these fits, the exponent ζ_{GaAs} can be determined as 3.0±0.2. These exponents/slopes are in rough agreement with the expected value, depicted as a line with slope ζ=3.3.

CONCLUSIONS

The study of the gecko adhesion system is a fascinating confluence of the biological and materials sciences. Our results support the hypothesis that changes in the materials properties produced by atmospheric moisture will alter the conditions for detachment of gecko setae. We measured significant changes in the viscoelastic response of β-keratin with atmospheric moisture, exemplified by a roughly 4-fold increase in the loss tangent. Enhanced dissipation in the material can have a profound influence on the energetics of the peeling of the contact, and can strengthen the interface between the gecko's foot structures and the underlying surface. Given the near-absence of adhesion below 15% RH (Fig. 1A), it is interesting to consider whether tokay geckos require the presence of atmospheric moisture for attachment, and whether gecko species from dry climates suffer from impaired adhesion in this regard. It has not escaped our notice that the performance of GSAs could be similarly enhanced using the same dissipative material behavior. Chemical modification of the GSA material could strengthen the individual fiber/substrate interfaces without sacrificing the benefits of a fibrillar structure.

Changes in materials properties, not capillary forces, explain the effects of humidity. We conclude that capillary forces are not a significant factor, and that van der Waals forces remain the only empirically supported mechanism of adhesion in geckos.

LIST OF SYMBOLS AND ABBREVIATIONS

A	cross-sectional area
c_1, c_2, c_3	non-linear fit parameters for $(E')^{-1}$
DMA	dynamic mechanical analysis
E, E', E''	complex modulus, storage modulus, loss modulus
E^*	contact modulus
F, F_a, F_f	applied force, adhesion force, frictional force
F_0	substrate-dependent factor in F_a
GSA	gecko-like synthetic adhesive
m, ζ	phenomenological exponents
o	asymptotically small terms in F_a
R	fiber radius
RH	relative humidity
t	time
t_{cap}	capillary bridge formation time
v	drag velocity
v_c	crack extension velocity
vdW	'van der Waals'
α	coefficient of highest order term in F_a
γ, γ_0, $\Delta\gamma$	work of adhesion, surface energy, viscoelastic contribution to work of adhesion
δ	loss angle
$\varepsilon(t)$, ε_0	dynamic strain, strain amplitude
ζ_{GaAs}, ζ_{SiO2}	empirical exponents
θ	contact angle
μ	coefficient of friction
ν	Poisson's ratio
σ, σ_a	stress applied to fiber, fiber pull-off stress
$\sigma(t)$, σ_0	dynamic stress, stress amplitude
τ	spatula slip timescale
Φ	multiplicative viscoelastic factor in work of adhesion
ω	frequency

ACKNOWLEDGEMENTS

We acknowledge Andrew Schnell at Lewis and Clark College for his assistance in specimen collection and preparation. We also thank Donald Stone at the University of Wisconsin – Madison and Ronald Fearing, Robert Full and Brian Bush at the University of California – Berkeley for discussion. This research was supported by the National Science Foundation under awards NBM 0900723 and IOS 0847953.

REFERENCES

Andrews, E. H. (1985). The role of viscoelasticity in adhesion. *J. Polym. Sci. Pol. Sym.* **72**, 295-297.

Aristotle (1910). *Historia Animalium*, Book IX. Oxford, UK: The Clarendon Press. Available online at http://classics.mit.edu/Aristotle/history_anim.mb.txt.

Autumn, K. and Peattie, A. M. (2002). Mechanisms of adhesion in geckos. *Integr. Comp. Biol.* **42**, 1081-1090.

Autumn, K., Liang, Y. A., Hsieh, S. T., Zesch, W., Chan, W. P., Kenny, T. W., Fearing, R. and Full, R. J. (2000). Adhesive force of a single gecko foot-hair. *Nature* **405**, 681-685.

Autumn, K., Sitti, M., Liang, Y. A., Peattie, A. M., Hansen, W. R., Sponberg, S., Kenny, T. W., Fearing, R., Isrealachvili, J. N. and Full, R. J. (2002). Evidence for van der Waals adhesion in gecko setae. *Proc. Natl. Acad. Sci. USA* **99**, 12252-12256.

Autumn, K., Dittmore, A., Santos, D., Spenko, M. and Cutkosky, M. (2006a). Frictional adhesion: a new angle on gecko attachment. *J. Exp. Biol.* **209**, 3569-3579.

Autumn, K., Majidi, C., Groff, R. E., Dittmore, A. and Fearing, R. (2006b). Effective elastic modulus of isolated gecko setal arrays. *J. Exp. Biol.* **209**, 3558-3568.

Bonser, R. H. C. (2002). Hydration sensitivity of ostrich claw keratin. *J. Mater. Sci. Lett.* **21**, 1563-1564.

Bonser, R. H. C. and Purslow, P. P. (1995). The Young's modulus of feather keratin. *J. Exp. Biol.* **198**, 1029-1033.

Chen, B. and Gao, H. (2010). An alternative explanation of the effect of humidity in gecko adhesion: stiffness reduction enhances adhesion on a rough surface. *Int. J. Appl. Mech.* **2**, 1-9.

Danilatos, G. D. and Postle, R. (1981). Dynamic mechanical properties of keratin fibers during water absorption and desorption. *J. Appl. Polym. Sci.* **26** 193-200.

Dellit, W.-D. (1934). Zur anatomie und physiologie der Geckozehe. *Jena Z. Naturw.* **68**, 613-656.

Federle, W. (2006). Why are so many adhesive pads hairy? *J. Exp. Biol.* **209**, 2611-2621.

Federle, W., Barnes, W. J. P., Baumgartner, W., Drechsler, P. and Smith, J. M. (2006). Wet but not slippery: boundary friction in tree frog adhesive toe pads. *J. R. Soc. Interface* **3**, 689-697.

Fisher, L. R. and Israelachvili, J. N. (1981). Direct measurement of the effect of meniscus forces on adhesion: a study of the applicability of macroscopic thermodynamics to microscopic liquid interfaces. *Colloids Surf.* **3**, 303-319.

Fraser, R. D. B. and Macrae, T. P. (1980). Molecular structure and mechanical properties of keratins. *Symp. Soc. Exp. Biol.* **34**, 211-246.

Fraser, R. D. B. and Parry, D. A. D. (1996). The molecular structure of reptilian keratin. *Int. J. Biol. Macromol.* **19**, 207-211.

Gao, H. and Yao, H. (2004). Shape insensitive optimal adhesion of nanoscale fibrillar structures. *Proc. Natl. Acad. Sci. USA* **101**, 7851-7856.

Gao, H., Wang, X., Yao, H., Gorb, S. and Arzt, E. (2005). Mechanics of hierarchical adhesion structures of geckos. *Mech. Mater.* **37**, 275-285.

Geim, A. K., Dubonos, S. V., Grigorieva, I. V., Novoselov, K. S., Zhukov, A. A. and Shapoval, S. Y. (2003). Microfabricated adhesive mimicking gecko foot-hair. *Nat. Mater.* **2**, 461-463.

Goodwyn, P. P., Peressadko, A., Schwarz, H., Kastner, V. and Gorb, S. (2006). Material structure, stiffness, and adhesion: why attachment pads of the grasshopper (*Tettigonia viridissima*) adhere more strongly than those of the locust (*Locusta migratoria*) (*Insecta*: *Orthoptera*). *J. Comp. Physiol. A* **192**, 1233-1243.

Gravish, N., Wilikinson, M. and Autumn, K. (2008). Frictional and elastic energy in gecko adhesive detachment. *J. R. Soc. Interface* **5**, 339-348.

Gravish, N., Wilkinson, M., Sponberg, S., Parness, A., Esparza, N., Soto, D., Yamaguchi, T., Broide, M., Cutkosky, M., Cretin, C. et al. (2010). Rate-dependent frictional adhesion in natural and synthetic gecko setae. *J. R. Soc. Interface* **7**, 259-269.

Griffith, A. A. (1921). The phenomena of rupture and flow in solids. *Philos. Trans. R. Soc. Lond. A* **221**, 163-198.

Hanna, G. and Barnes, W. J. P. (1991). Adhesion and detachment of the toe pads of tree frogs. *J. Exp. Biol.* **155**, 103-125.

Hansen, W. R. and Autumn, K. (2005). Evidence for self-cleaning in gecko setae. *Proc. Natl. Acad. Sci. USA* **102**, 385-389.

Huber, G., Mantz, H., Spolenak, R., Mecke, K., Jacobs, K., Gorb, S. N. and Artz, E. (2005). Evidence for capillary contributions to gecko adhesion from single spatula nanomechanical measurements. *Proc. Natl. Acad. Sci. USA* **102**, 16293-16296.

Huber, G., Gorb, S. N., Hosoda, N., Spolenak, R. and Arzt, E. (2007). Influence of surface roughness on gecko adhesion. *Acta Biomater.* **3**, 607-610.

Hui, C.-Y., Xu, D.-B. and Kramer, E. J. (1992). A fracture model for a weak interface in a viscoelastic material (small scale yielding analysis). *J. Appl. Phys.* **72**, 3294-3304.

Israelachvili, J. (1992). *Intermolecular and Surface Forces.* San Diego, CA: Academic Press.

Kendall, K. (1979). The connection between fracture energy and inelastic behaviour. *Acta Metall.* **27**, 1065-1073.

Kim, T. W. and Bhushan, B. (2008). The adhesion model considering capillarity for gecko attachment system. *J. R. Soc. Interface* **5**, 319-327.

Lee, J., Bush, B., Maboudian, R. and Fearing, R. S. (2009). Gecko-Inspired combined lamellar and nanofibrillar array for adhesion on nonplanar surface. *Langmuir* **25**, 12449-12453.

Maderson, P. F. A. (1964). Keratinized epidermal derivatives as an aid to climbing in gekkonid lizards. *Nature* **203**, 780-781.

Mahdavi, A., Ferreira, L., Sundback, C., Nichol, J. W., Chan, E. P., Carter, D. J. D., Bettinger, C. J., Patanavanich, S., Chignozha, L., Ben-Joseph, E. et al. (2008). A biodegradable and biocompatible gecko-inspired tissue adhesive. *Proc. Natl. Acad. Sci. USA* **105**, 2307-2312.

McFarlane, J. S. and Tabor, D. (1950). Adhesion of solids and the effect of surface films. *Proc. R. Soc. Lond. A* **202**, 224-243.

Murphy, M. P., Aksak, B. and Sitti, M. (2007). Adhesion and anisotropic friction enhancements of angled heterogeneous micro-fiber arrays with spherical and spatula tips. *J. Adhes. Sci. Technol.* **21**, 1281-1296.

Niewiarowski, P. H., Lopez, S., Ge, L., Hagen, E. and Dhinojwala, A. (2008). Sticky gecko feet: the role of temperature and humidity. *PLoS ONE* **3**, e2192.

Persson, B. N. J. (2003). On the mechanism of adhesion in biological systems. *J. Chem. Phys.* **118**, 7614-7621.

Pesika, N. S., Zeng, H., Kristiansen, K., Zhao, B., Tian, Y., Autumn, K. and Israelachvili, J. (2009). Gecko adhesion pad: a smart surface? *J. Phys. Condens. Matter* **21**, 464132.

Rizzo, N. W., Gardner, K. H., Walls, D. J., Keiper-Hrynko, N. M., Ganzke, T. S. and Hallahan, D. L. (2006). Characterization of the structure and composition of gecko adhesive setae. *J. R. Soc. Interface* **3**, 441-451.

Ruibal, R. and Ernst, V. (1965). The structure of the digital setae of lizards. *J. Morphol.* **117**, 271-293.

Russell, A. P. (2002). Integrative functional morphology of the gekkotan adhesive system (*Reptilia*: *Gekkota*). *Integr. Comp. Biol.* **42**, 1154-1163.

Russell, A. P. and Johnson, M. K. (2007). Real-world challenges to, and capabilities of, the gekkotan adhesive system: contrasting the rough and the smooth. *Can. J. Zool.* **85**, 1228-1238.

Saulnier, F., Ondarçuhu, T., Aradian, A. and Raphaël, E. (2004). Adhesion between a viscoelastic material and a solid surface. *Macromolecules* **37**, 1067-1075.

Sitti, M. and Fearing, R. S. (2003). Synthetic gecko foot-hair micro/nano-structures as dry adhesives. *J. Adhes. Sci. Technol.* **17**, 1055-1073.

Sun, W., Neuzil, P., Kustandi, T. S., Oh, S. and Samper, V. D. (2005). The nature of the gecko lizard adhesive force. *Biophys. J.* **89**, L14-L17.

Szoszkiewicz, R. and Riedo, E. (2005). Nucleation time of nanoscale water bridges. *Phys. Rev. Lett.* **95**, 135502.

Taylor, A. M., Bonser, R. H. C. and Farrent, J. W. (2004). The influence of hydration on the tensile and compressive properties of avian keratinous tissue. *J. Mater. Sci.* **39**, 939-942.

Thomson, W. (1871). On the equilibrium of a vapour at a curved surface of liquid. *Phil. Mag.* **42**, 448-452.

Yamaguchi, T., Gravish, N., Autumn, K. and Creton, C. (2009). Microscopic modeling of the dynamics of frictional adhesion in the gecko attachment. *J. Phys. Chem. B* **113**, 3622-3628.